

# Optimization of deposition parameters for thin film lithium phosphorus oxynitride (LIPON)

B. Uzakbaiuly<sup>\*,1</sup>, A. Mukanova<sup>2</sup>,  
I. Kurmanbayeva<sup>1</sup>, Z.B. Bakenov<sup>1,2,3</sup>

<sup>1</sup>National Laboratory Astana, Nur-Sultan, Kazakhstan

<sup>2</sup>Nazarbayev University, Nur-Sultan, Kazakhstan

<sup>3</sup>Institute of Batteries LLP, Nur-Sultan, Kazakhstan

E-mail: berik.uzakbaiuly@nu.edu.kz

DOI: 10.29317/ejpfm.2019030209

Received: 11.06.2019 - after revision

Thin film of lithium phosphorus oxynitride (LIPON) was successfully deposited by radio frequency (RF) magnetron sputtering technique using a  $\text{Li}_3\text{PO}_4$  target. The optimal deposition parameters were determined for the thin films with the highest target-substrate distance. Characterization of deposited film was carried out by AFM, FTIR and Raman spectroscopy, which showed incorporation of nitrogen into the film as both doubly,  $\text{N}_d$ , and possibly triply,  $\text{N}_t$ , coordinated form. The ac impedance spectroscopy measurements revealed that the highest ionic conductivity of  $1.1 \mu\text{Scm}^{-1}$  was achieved at room temperature for the samples prepared at the optimum RF power and gas flow conditions.

**Keywords:** thin film, LIPON, RF sputtering, PVD.

## Introduction

On a verge of various energy harvesting solutions such as solar cells, thermoelectric and piezoelectric devices, there is a need for a reliable energy storage solutions. Thin film battery technology is considered to be promising route because of its small size, high energy density and long cycle life. Possible uses of these batteries are in microelectronics with a capability of on chip design, medical implant devices, radio-frequency identification (RFID) tags, and future internet

of things (IoT) devices. Future thin film batteries are all solid state batteries manufactured by various techniques. One of these techniques is physical vapor deposition (PVD).

Table 1.

Comparison of ionic conductivities ( $\sigma$ ) by different groups (chronological order).

Author	Power density (W/cm <sup>2</sup> )	N <sub>2</sub> Pressure (Pa)	Target-substrate distance (cm)	Ionic conductivity ( $\mu\text{Scm}^{-1}$ )
Bates et al. (1992) [2]	6.91	2.6	5	2.2
Choi et al. (2002) [12]	0.98	0.8	*	1.67
Park et al. (2006) [14]	2.22	0.67	12	0.895
Hamon et al. (2006) [15]	2.3	1	7.5	1.8
Hu et al. (2008) [8]	5.5	1.5	6	3.3
Nimisha et al. (2011) [16]	3	*	4	1.1
Lethien et al. (2011) [17]	1.85	*	7	1.5
Fleutot et al. (2011) [10]	2	1	8	3.1
Li et al. (2014) [9]	5.5	1.5	*	2.3
Kovalenko et al. (2014) [11]	2.2	1.33	4	3.2
Su et al. (2015) [7]	2.19	0.15	5.3	4.9
Vieira et al. (2016) [18]	4.93	0.1	7.5	0.27

\* not indicated in the paper

An important 'layer' component of a stable solid state battery is a solid electrolyte [1]. Solid electrolytes do not only act as Li-ion conductor, but they also act as separators to prevent Li dendrite growth and electrical short-circuiting. Among them lithium phosphorus oxynitride ( $\text{Li}_3\text{PO}_4\text{N}_x$ , LIPON) is regarded as an electrolyte, stable upon operation with lithium (0-5 V Li/Li<sup>+</sup>) and possessing relatively high ionic conductivity ( $\sim 10^{-6} \text{ Scm}^{-1}$ ) [2-10]. LIPON first was investigated as a solid electrolyte at the Oak Ridge National Laboratory, and was grown by radio frequency magnetron sputtering (RF MS) [2]. Other techniques such as ion-beam assisted deposition (IBAD) [3], pulsed laser deposition (PLD) [4], atomic

layer deposition (ALD) [5], and chemical vapor deposition (CVD) [6] have been investigated to enhance its ionic conductivity. However, RF MS has been used for the highest reported value of ionic conductivity ( $4.9 \mu\text{Scm}^{-1}$ ) [7].

Various groups have reported RF MS preparation of LIPON electrolyte (See Table 1). Properties of the solid electrolyte highly depend on parameters of the deposition such as deposition power, target-substrate distance, flow of  $\text{N}_2$  gas, pressure, base pressure before deposition. As can be seen from Table 1, similar deposition parameters show contradictory behaviors. For instance, it has been reported by Hu et al. that at nitrogen ( $\text{N}_2$ ) pressure of 1.5 Pa and power density of  $5.5 \text{ W/cm}^2$ , the ionic conductivity ( $\sigma$ ) of LIPON solid electrolyte is  $3.3 \mu\text{Scm}^{-1}$  [8].

Contrary to that, Li et al. found  $\sigma$  to be  $2.3 \mu\text{Scm}^{-1}$ , for the same  $\text{N}_2$  pressure and power density [9]. The only difference in deposition parameter was target-substrate distance. Large target-substrate distance could lead to reaction of nitrogen with  $\text{Li}_3\text{PO}_4$  target and cause the target to disintegrate or become acidic. This phenomenon led to observation of lower value of ionic conductivity by Li et al. Although several groups reported close  $\sigma$  values, they show very broad variation of power densities, target-substrate distances and  $\text{N}_2$  pressures. For example, Hu et al., Fleutot et al., and Kovalenko et al. observed  $\sigma$ 's around  $3 \mu\text{Scm}^{-1}$ , but all have differences in the deposition parameters (Table 1) [8, 10, 11].

Many of groups deposited LIPON with target-substrate distance of 12 cm or less. The high inconsistency in deposition parameters and ionic conductivities shows that there are other factors that affect the resulting LIPON layer characteristics. Therefore, it is important that the parameters are optimized for the large target-substrate distance and large chamber. In this paper, we investigate various conditions for successfully depositing LIPON electrolyte on glass substrate with the highest target-substrate distance of 18 cm reported to date. Ionic conductivities of LIPON were determined through electrochemical impedance spectroscopy and were analyzed.

## Experimental section

Magnetron sputtering technique has been used to deposit LIPON on several glass substrates. Sputter target, lithium phosphate  $\text{Li}_3\text{PO}_4$  (Kurt J Lesker), of 99.95% purity were  $\sim 5$  cm in diameter and  $\sim 0.64$  cm in thickness. Before each deposition, the chamber was pumped down to  $9.3 \times 10^{-5}$  Pa pressure using turbomolecular pump. Samples were grown in nitrogen environment (99.99% purity) at chamber pressures indicated in Table 2, and nitrogen flow varying from 10-24 sccm. The power has been changed from 60-200 W so as to look at different ionic conductivity values and spectroscopic characterization. Samples were investigated by Fourier Transform Infrared (FTIR) (Nicolet iS10 FT-IR) spectroscopy between frequencies of  $400\text{-}3000 \text{ cm}^{-1}$  and Raman (Horiba LabRam Evolution) spectroscopy between frequencies of  $300\text{-}2500 \text{ cm}^{-1}$  to validate the nitrogen incorporation. For FTIR measurements, samples were deposited onto Si substrate ( $\sim 1$  mm) since it has weak multi-phonon absorption in the frequency

region investigated. The samples were deposited on Si substrate because the glass absorbs below  $1000\text{ cm}^{-1}$  range and would obscure the observation of nitrogen vibrational modes. Atomic force microscopy (AFM) (SmartSPM 1000) was used to study the morphology of the samples and to estimate the thicknesses of sputtered LIPON films. In this experiment, the tip of the probe was scanned through the edge of the film. The probe cantilever had root-mean-square sensitivity of  $<0.04\text{ nm}$ . AC impedance spectroscopy (ACIS) was conducted using VMP3 Biologic with LIPON electrolyte sandwiched between two blocking copper or chromium electrodes (Glass/M/LIPON/M). In order to obtain such structure first metal, then LiPON, and then metal were deposited using DC, RF, and DC sputtering respectively. The frequency range of the ACIS measurement was from 1 Hz to 1 MHz, with the sinus amplitude of applied voltage of 10 mV.

## Results and Discussion

Samples with various deposition conditions are shown in Table 2. The Raman data (Figure 1) revealed the nitrogen incorporation into the film in both doubly,  $N_d$ , and, triply  $N_t$ , coordinated form. Absorption peaks due to P-N=P, P-N<P<sub>2</sub> and P-O vibrational modes could be observed in Raman spectra at  $630\text{ cm}^{-1}$ ,  $720\text{ cm}^{-1}$  and  $1100\text{ cm}^{-1}$  respectively [5, 12]. For samples deposited at higher sputtering power and nitrogen pressure, more features due to nitrogen incorporation could be observed. Sample deposited at 60 W target power (green) shows more intensified P-O bonding vibration than sample deposited at 150 W target power (pink). This is because the P-O vibrations get to be replaced by P-N vibrational modes in 150 W sample. In addition, peaks in infrared spectra (Figure 2) were observed by FTIR spectrometer and were assigned to Li-O-P, P-O, P-N vibrational modes. Deposition for a longer period results in higher absorption in infrared spectrum which indicates higher nitrogen content in the LIPON electrolyte. These results indicate successful incorporation of nitrogen into the film. Recently, Lacivita et al. reported that the usual identification of  $N_t$  is incorrect (i.e., N does not bridge three phosphate units) and that the N atoms are most probably non-bridging apical N ( $N_a$ , i.e., N is in isolated P(O,N)<sub>4</sub> tetrahedra) [13]. Further Raman and FTIR investigation for correlating  $N_d$ ,  $N_t$ ,  $N_a$  vibrational modes are beyond the scope of this work.

The thicknesses of LIPON electrolytes were determined through AFM and are shown in Table 2. Figure 3 shows AFM picture of two LIPON films which were deposited at two different conditions. The one deposited for 7 hours and the one deposited for 16 hours. It is seen that samples deposited during a longer deposition time have very uneven surface. This lack of uniformity is attributed to the fact that sputtered atoms have to travel long distance before reaching substrate.

Ionic conductivities are shown in Table 2 for the samples that did not short circuit. The ionic conductivity was determined using the formula

$$\sigma = \frac{d}{R_2 A}, \quad (1)$$

where  $R_2$  is resistivity,  $A$  is the sandwiched area of LIPON film that is in between

Table 2.

RF magnetron deposition of LIPON.

Assemble type	Power (W); [PD] (W/cm <sup>2</sup> )	N <sub>2</sub> Pressure (Pa)	Deposition Time (h)	Thickness of Lipon $d$ (nm)	Result; Resistance	Note
Glass-Cu- Lipon-Cu	60; [2.96]	0.07	10	4100±310	Shorts	Cu was evaporated at: P = 100 W, Argon pressure ( $P_{Ar}$ ) = 0.67 Pa, time = 10 min, thickness unknown
Glass-Cu- Lipon-Cu	70; [3.45]	0.07	12	-	Shorts	Cu: P = 70 W, t=15 min, $P_{Ar}$ = 0.67 Pa, thickness unknown
Cu foil-Lipon- Cu	70; [3.45]	0.67	5	380±80	Shorts	Cu: P = 100 W, $P_{Ar}$ = 0.67 Pa, t = 20 min, thickness = 410±30 nm
Glass-Cu-Cr- Lipon-Cr-Cu	80; [3.95]	0.13	7	370±40	Shorts	Cr was evaporated: P = 100 W $P_{Ar}$ = 0.67 Pa, t = 10 min, thickness = 180±5 nm
Si-Lipon	90; [4.44]	0.67	3.5	240±80	NA	Sputtered for FTIR measurement
Glass-Cu- Lipon-Cu	100; [4.93]	0.13	16	2640±420	Insulates; R=3090 $\Omega$	Sandwiched area ( $A$ ) = $\pi \times (8\text{mm})^2 = 2 \text{ cm}^2$ , Ionic conductivity $\sigma = 0.042 \mu\text{Scm}^{-1}$
Glass-Cr-Lipon- Cr	100; [4.93]	0.67	3	380±20	Insulates; R=1087 $\Omega$	$A = 1.8 \text{ mm} \times 2 \text{ mm} = 3.6 \text{ mm}^2$ , $\sigma = (0.97 \pm 0.05) \mu\text{Scm}^{-1}$
Glass-Cu-Cr- Lipon-(Ni paste)	150; [7.4]	0.27	10	1480±330	Insulates; R=2.05 M $\Omega$	Partial nitrogen pressure: Ar/N <sub>2</sub> ratio $\approx 1/3$ , $A =$ , $\sigma = 0.0009 \mu\text{Scm}^{-1}$
Glass-Cr-Lipon- Cr	150; [7.4]	0.67	3	720±80	Shorts	$A = 2 \text{ mm} \times 2 \text{ mm} = 4\text{mm}^2$
Glass-Cr-Lipon- Cr	200; [9.87]	0.67	3	900±60	Insulates; R=2038 $\Omega$	$A = 2 \text{ mm} \times 2 \text{ mm} = 4\text{mm}^2$ , $\sigma = (1.1 \pm 0.07) \mu\text{Scm}^{-1}$

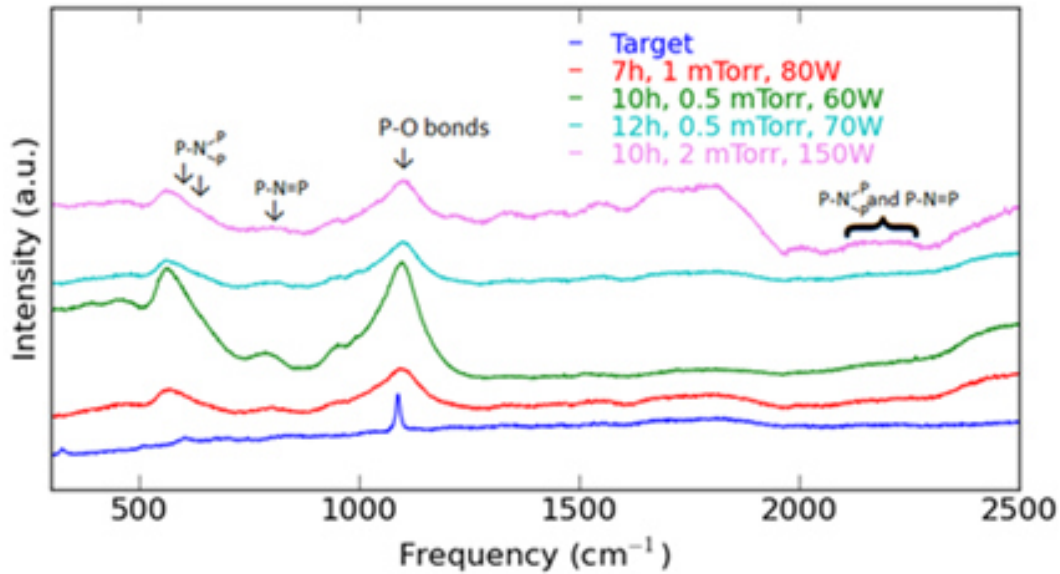


Figure 1. Raman spectra of LIPON thin film deposited at different parameter settings for some of the samples in the Table 2.

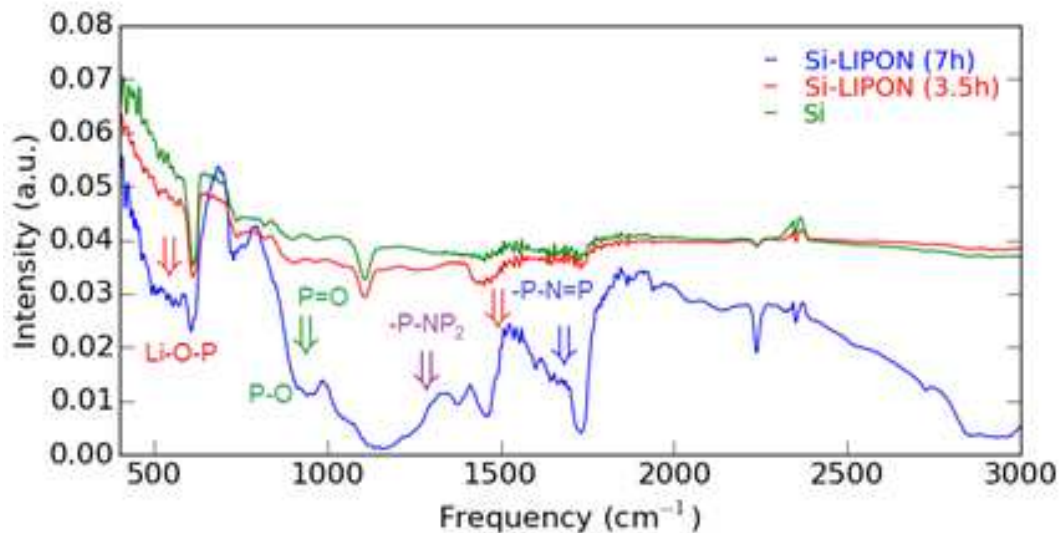


Figure 2. FTIR spectra of Si, Si-LIPON (3.5 h deposition), Si-LIPON (7 h deposition) for samples in the Table 2.

two blocking electrodes, and  $d$  is the thickness of the film. Figure 4 shows Nyquist plot of the sample (deposited at 200 W power) with no short-circuiting. This sample exhibits a resistance of about 2038 Ohms which was estimated from the fit to the data. Resistances for other samples were determined in similar manner.

The ionic conductivities for the best samples were calculated as  $1.1 \mu\text{Scm}^{-1}$  and  $0.97 \mu\text{Scm}^{-1}$  for samples deposited with target power at 100 W and 200 W respectively. The ionic conductivity obtained ( $1.1 \mu\text{Scm}^{-1}$ ) is comparable to the highest values reported and paves the way for future LIPON deposition [2, 7-18].

Other samples that did not short circuit include samples deposited at 100 W, 0.13 Pa and 150 W, 0.27 Pa which showed ionic conductivities of  $0.04 \mu\text{Scm}^{-1}$  and  $0.0009 \mu\text{Scm}^{-1}$  respectively. This is very low compared to the above values and reason for such low  $\sigma$  might be because of low  $\text{N}_2$  pressure used for the former and mixture of  $\text{Ar}/\text{N}_2$  gas used for the latter sample.

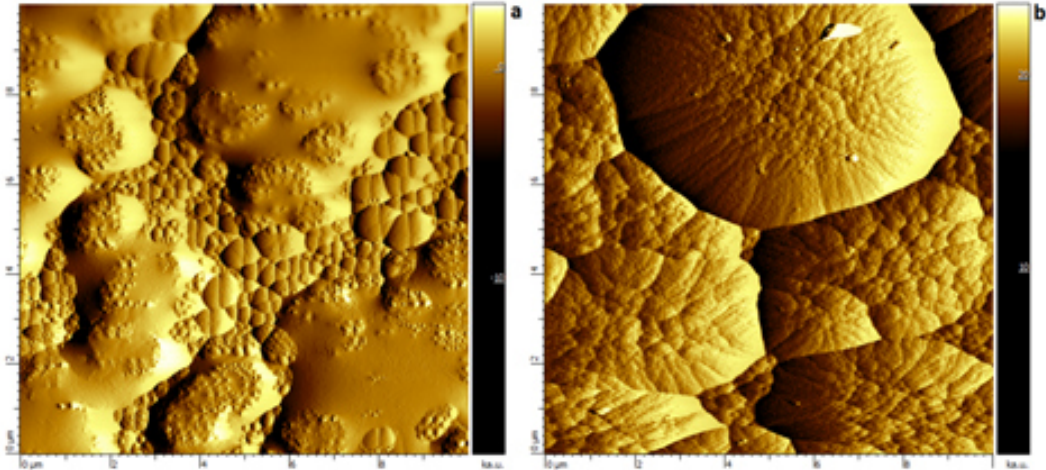


Figure 3. AFM images of a) 7 h and b) 16 h deposited LIPON electrolyte on substrates described in the Table 2.

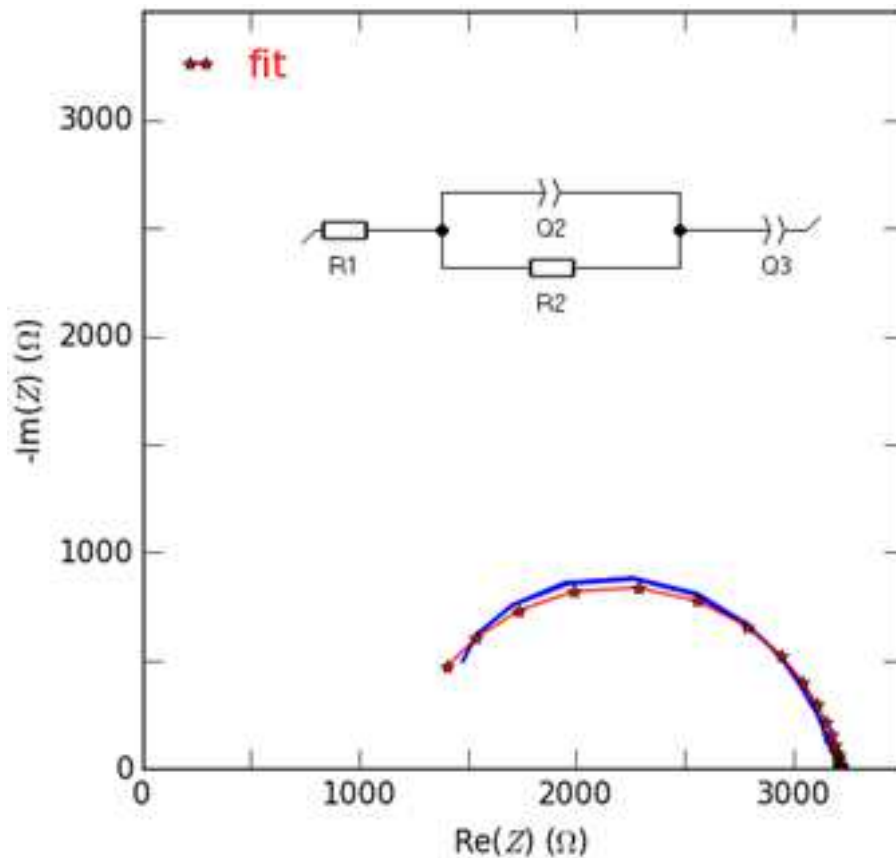


Figure 4. Nyquist plot of sample G-Cr-LIPON-Cr 3 h (200 W) Inset: Equivalent circuit used to fit the experimental data.

It should be noted that higher  $N_2$  pressures (1.33 Pa) resulted in no deposition of electrolyte and increasing power resulted in target etching instead of deposition on the substrate. Also, as can be seen from Table 2, although having similar power densities to reported values in Table 1, several samples that were sandwiched between blocking electrodes were short-circuited. This could be the result of high unevenness of deposited samples as it was shown by AFM (Figure 3). Short circuiting of the LIPON electrolyte has also been observed by Vieira et al [18]. The group attributes this to dielectric breakdown happening when voltage difference between two blocking electrodes is too high. Simply, high unevenness creates

regions with very thin layers of electrolyte and when voltage difference is applied to electrodes, dielectric breakdown happens and sample shorts. The reason for unevenness of deposited layer might be because of large target-substrate distance we have in our system. Large target-substrate distance makes the deposition to become non-uniform as the resulting fluxes of atoms are distributed unevenly. This behavior is particularly interesting to note because the different deposition parameters and volume of chamber are critical in future mass production of thin film batteries.

## Conclusion

We have fabricated thin films of LIPON solid electrolyte at large target-substrate distance ( $\sim 18$  cm) which showed the best ionic conductivity of  $1.1 \mu\text{Scm}^{-1}$ . The optimal deposition condition for our system was 200 W target power ( $9.87 \text{ W/cm}^2$  power density) and 100%  $\text{N}_2$  media. Power densities with lower values ( $< 4 \text{ W/cm}^2$ ) result in sample dielectric breakdown upon ac impedance measurements. Low FTIR and Raman spectra showed the nitrogen incorporation into the solid electrolyte. Potential thin film battery based on this solid electrolyte will be fabricated in the future.

## Acknowledgments

This research was funded under the research grant AP05133519 "Development of 3-dimensional thin film silicon based anode materials for next generation lithium-ion microbatteries" from the Ministry of Education and Science of the Republic of Kazakhstan.

## References

- [1] Y. Masaki, Lithium-Ion Batteries, (Heidelberg, New York: Springer-Verlag, 2009) 47 p.
- [2] J.B. Bates et al., Soli. Stat. Ionc., **53-56** (1992) 647.
- [3] F. Vereda, Elec. and Soli.-Stat. Lett., **5**(11) (2002) A239.
- [4] N. Kuwata, ECS Tran., **16**(26) (2009) 53.
- [5] A.C. Kozen, Chem. of Mater., **27**(15) (2015) 70.
- [6] H.T. Kim, Jour. of Pow. Sour., **244** (2013) 641.
- [7] Y. Su, Soli. Stat. Ionc., **282** (2015) 63.
- [8] Z. Hu, Bull. Mater. Sci., **31**(4) (2008) 681.
- [9] D. Li, Mater. Lett., **134** (2014) 237.
- [10] B. Fleutot, Soli. Stat. Ionc., **186** (2011) 29.
- [11] L. Kovalenko, IEEE International Scientific Conference Electronics and Nanotechnology, Kiyv **34** (2014) 126.
- [12] C.H. Choi, Elec. and Soli.-Stat. Lett., **5**(1) (2002) A14.
- [13] V. Lacivita, Jour. of the Amer. Chem. Soc., **140**(35) (2018) 11029.



- [14] H.Y. Park, Jour. Elec., **17** (2006) 1023.
- [15] Y. Hamon, Soli. Stat. Ionc., **177** (2006) 257.
- [16] C.S. Nimisha, Thin Soli. Film., **519** (2011) 3401.
- [17] C. Lethien, Micr. Eng., **88** (2011) 3172.
- [18] E.M.F. Vieira, Jour. of Phys. D **49** (2016) 70.